HHS Public Access

Author manuscript

Int Forum Allergy Rhinol. Author manuscript; available in PMC 2019 April 01.

Published in final edited form as:

Int Forum Allergy Rhinol. 2018 April ; 8(4): 513–521. doi:10.1002/alr.22072.

Characterization of a novel, papain inducible murine model of eosinophilic rhinosinusitis

Anuj Tharakan, BS[1], **Alex Dobzanski, MS**[1], **Nyall R. London Jr., MD, PhD**[1], **Syed M. Khalil, PhD**[1], **Nitya Surya**[1], **Andrew P. Lane, MD**[1], and **Murugappan Ramanathan Jr., MD, FACS**[1]

[1]Department of Otolaryngology-Head and Neck Surgery, Johns Hopkins University School of Medicine Baltimore, MD

Abstract

Background—Eosinophilic chronic rhinosinusitis (ECRS) is a disease characterized by eosinophilic inflammatory infiltrate and a local type 2 cytokine milieu. Current animal models fail to recapitulate many of the innate and adaptive immunological hallmarks of the disease, thus hindering the development of effective therapeutics. In the present study, mice were exposed intranasally to the cysteine protease papain, which shares functional similarities with parasitic proteases and aeroallergens, to generate a rapidly inducible murine model of eosinophilic rhinosinusitis.

Methods—C57BL/6 mice were intranasally instilled with 20 μg papain or heat inactivated papain (HP) on days 0–2 and days 7–10 and sacrificed on day 11. Nasal lavage fluid (NALF) was analyzed to quantify eosinophils and inflammatory cytokine secretion. Sinonasal tissue was sectioned and stained for goblet cells or homogenized to analyze cytokine levels. Serum samples were assayed for IgE by ELISA. Sinonasal mucosal tissue was dissociated and analyzed by flow cytometry.

Results—Compared to HP treated mice, papain treatment induced significant eosinophilia in NALF, goblet cell hyperplasia, innate and adaptive immune cell infiltration, type 2 cytokine production and IgE responses. Flow cytometric analysis of sinonasal tissues revealed significant inflammatory cell infiltration and IL-13 producing cell populations.

Conclusions—In this study, we demonstrate that the cysteine protease papain induces allergic sinonasal eosinophilic rhinosinusitis and resembles Th2 inflammation and innate immune characteristics of ECRS. This model permits further study into the molecular mechanisms underlying ECRS pathology and provides a model system for the evaluation of potential pharmacological interventions.

Corresponding Author: Murugappan Ramanathan Jr, MD, Department of Otolaryngology-Head and Neck Surgery, Johns Hopkins Outpatient Center, 601 N. Caroline St, 6th Floor, 6263, Baltimore, MD 21287, mramana3@jhmi.edu.

Disclosures: N.R.L. is a patent co-inventor for methods treating vascular barrier dysfunction licensed to Navigen Pharmaceuticals which is unrelated to papain and allergy. N.R.L. holds a small amount of stock in Navigen Pharmaceuticals which is currently of no value.

Presented at the ARS meeting at the AAOHNS on September 8–9, 2017

Keywords

Papain; rhinosinusitis; IL-33; epithelial barrier

Introduction

Chronic sinonasal inflammatory disease affects roughly 16% of the population in the United States and has detrimental effects on patients' quality of life [1]. Eosinophilic chronic rhinosinusitis (ECRS) is a chronic inflammatory disease of the nasal and paranasal sinuses which is characterized by eosinophilic inflammatory infiltrate and local production of the type 2 cytokines IL-4, IL-5, and IL-13 [2, 3]. Presently, the underlying pathophysiology of ECRS remains unclear and as a result, molecular targets for effective therapies have yet to be identified.

The identification of these molecular targets would be greatly facilitated by the development of a physiologically relevant model of ECRS. Most current models fail to effectively recapitulate many of the pathophysiological features of chronic rhinosinusitis (CRS), but rather produce a phenotype resembling eosinophilic rhinosinusitis. A commonly used murine model of eosinophilic rhinosinusitis is the ovalbumin model [4]. Although this model is characterized by robust allergic inflammation, it is entirely dependent on Th2 cells and IgE production. ECRS, conversely, often presents in the absence of allergen-specific IgE. The reliance of the ovalbumin model on the adaptive arm of the immune system therefore limits its translational utility because it fails to recapitulate the contribution of innate immune responses in eosinophilic rhinosinusitis and eosinophilic disease [3, 5].

Another frequently used murine model is the ovalbumin-staphylococcal enterotoxin B (SEB) model [6, 7]. This model utilizes the superantigen staphylococcus enterotoxin B to enhance allergic inflammatory responses in the ovalbumin model. A significant advantage to this model is its capacity to generate significant polypoid lesions which resemble the clinical course of CRS with nasal polyps. This model, similar to the ovalbumin model, is reliant on adaptive immune mechanisms resulting from superantigen-mediated polyclonal T cell activation and systemic immunization. To date, contributions of innate immune cells such as type 2 innate lymphoid cells (ILC2s), basophils, and mast cells have not been described in this model. Some murine models of eosinophilic rhinosinusitis utilize common environmental allergens such as house dust mite, cockroach, or *Alternaria alternata* antigens [8–10]. In these models, similar to the model we describe in this study, sensitization is induced via the airway rather than intraperitoneal allowing for a physiologically relevant mechanism of induction of type 2 airway inflammation. This permits the induction and involvement of innate immune pathways in the sinonasal epithelium which is a central feature of eosinophilic rhinosinusitis [3]. These models, however, activate allergen-specific immune pathways due to the presence of immunogenic fungal components associated with mites and insect allergens [11, 12]. Though these fungal pattern recognition pathways efficiently promote robust inflammation, they are not considered significant contributors to eosinophilic rhinosinusitis. The house dust mite-induced rhinitis model has also been used in conjunction with SEB treatments generating a phenotype similar to that of the OVA/SEB

model previously mentioned [13]. This model, however, requires systemic immunization and an adjuvant, and therefore has many of the drawbacks associated with the aforementioned models. Another problem with these models is the lot to lot variability in allergen extracts which leads to variable immune responses and difficulty with reproducibility.

Animal models of eosinophilic rhinosinusitis have also been established in rabbits and sheep [14–17]. Rodents have markedly different sinonasal anatomy from humans, making the rabbit and sheep models an attractive option to model sinus disease. The drawback to these models, however, is the lack of tools for genetic modification in these animals. This limits the capacity to conduct studies aimed at dissecting molecular mechanisms of ECRS pathophysiology. With these shortcomings in mind, we sought to generate an inducible murine model of eosinophilic rhinosinusitis to effectively model the innate and adaptive immune responses that characterize the disease pathology.

Emerging evidence indicates that damage to the sinonasal epithelial barrier plays a central role in eosinophilic rhinosinusitis pathogenesis [2, 3]. Injury to the epithelium has been implicated as a potential checkpoint in the secretion of the alarmin IL-33 which is integral to the initiation of type 2 inflammation [18]. Epithelial barrier disruption has been reported to occur in response to a variety of environmental agents as well as endogenous cytokines [19–23]. Interestingly, many aeroallergens with type 2 inflammation inducing properties demonstrate detectable protease activity [24]. This capacity to induce type 2 inflammation may be driven by proteolytic cleavage of intercellular junction between epithelial cells, thereby disrupting the barrier and subsequently causing epithelial cytokine release.

In this study, we developed an experimental model of eosinophilic rhinosinusitis by intranasal administration of the cysteine protease papain. We demonstrate that the cysteine protease activity of papain is essential to its ability to activate type 2 immune pathways in the murine sinonasal mucosa via epithelial disruption and IL-33 release. We show that this induction of IL-33 release results in type 2 inflammation which is characteristic of eosinophilic rhinosinusitis pathology.

Methods

Mice

Male and female C57BL/6 mice were obtained from Jackson Laboratories (Bar Harbor, ME). Animals were housed in a specific pathogen-free facility with single ventilated cages. All animal experiments were approved by the Johns Hopkins Institutional Animal Care and Use Committee.

In vivo treatments

To induce sinonasal inflammation, mice were anaesthetized and treated intranasally with 20 μg of papain (Sigma-Aldrich, St. Louis, MO Cat# P5306-25MG) in a 20 μl volume of PBS. For mice treated with heat-inactivated papain (HP), the papain solution was boiled at 95°C for 30 minutes and allowed to cool prior to intranasal treatment. Mice were treated on days 0–2 and days 7–11 (Figure 1a) and were sacrificed 24 hours after the final treatment unless otherwise stated. This dosing scheme was adapted from previously published papain-

induced murine models of asthma [25, 26]. We observed no adverse health effects such as weight loss or changes in food or water intake at the 11-day time point.

Nasal lavage and cytology

Transpharyngeal nasal airway lavage fluid (NALF) was collected as previously described [27]. Nasal lavage fluid was centrifuged at 500xg for 5 minutes. Supernatants were collected and analyzed for cytokine levels. Cell pellets from lavage samples were re-suspended in 100 μl PBS with 2 mM EDTA and total cells were counted manually using a hemocytometer. Cytospin slides were prepared using the StatSpin Cytofuge 12 (Beckman Coulter, Brea, CA) and stained with Diff-Quik stain (Dade Behring-Switzerland, Deerfield, IL), followed by a differential count of at least 200 cells per slide.

Sinonasal histopathology

Mice were anesthetized and transcardially perfused with phosphate buffered saline (PBS) until systemic blood was cleared. Mice were then perfused with cold 4% paraformaldehyde. The upper airway, including palatopharyngeal region, was isolated by scissor dissection, and the mouse head was separated at the level of the larynx and the hard palate was removed. The mouse heads were fixed in 4% paraformaldehyde overnight, washed, and decalcified in TBD-2 (Thermo Fisher Scientific, Waltham, MA) and embedded in optimum cutting temperature compound (Tissue Tek, Torrance, CA). Mouse sinonasal tissue cryosectioned and stained with Alcian blue-Nuclear fast red.

Flow cytometry

Mouse sinonasal tissue was isolated as described above and were minced and incubated for 45 minutes in 6 ml of dissociation buffer consisting of RPMI 1640, penicillin/streptomycin, β-mercaptoethanol, 0.2 mg/ml DNase I (Sigma Aldrich, St. Louis, MO), and 50 μg/ml Liberase TL (Roche Diagnostics, Indianapolis, IN). To make a single-cell suspension, the tissue was forced through a 70 μm cell strainer. Dissociation was stopped by the addition of 600 μl of fetal bovine serum. Cells were stained with Zombie Aqua fixable viability dye (Biolegend, San Diego, CA) prior to immunostaining.

For intracellular cytokine staining, single-cell suspensions were incubated 12 hours in 50 ng/ml phorbol 12-myristate 13-acetate (PMA) and 1 mM ionomycin. Cells were treated with 3 μg/ml brefeldin A for the final 3 hours of the stimulation.

Tissue cytokines

Nasal septa, nasoturbinates, and maxillary turbinates were excised from mice and snap frozen. Tissues were then suspended in PBS containing 0.1% Triton X-100, c0mplete mini protease inhibitor (Roche Diagnostics, Indianapolis, IN), and 1 mM PMSF. Tissue was homogenized and centrifuged for 2 minutes at 15,000xg. Supernatants were collected and analyzed for IL-4, IL-5 and IL-13 concentration by ELISA (R&D Systems, Minneapolis, MN). 100 μg of protein was loaded per well.

Nasopharyngeal associated lymphoid tissue restimulation

Nasopharyngeal associated lymphoid tissue (NALT) was isolated from the hard palate as previously described [28]. These cell suspensions were suspended in RPMI 1640 medium supplemented with 5% fetal bovine serum, penicillin/streptomycin, and β-mercaptoethanol with 20 μg/ml HP for 3 days. Culture supernatants were collected and analyzed for IL-4, IL-5, and IL-13 by ELISA.

Serum IgE

Blood was collected by cardiac puncture and serum was isolated using BD microtainer tubes (Becton Dickinson Biosciences, Franklin Lakes, NJ) using the manufacturer's protocol. Total IgE was assayed by sandwich ELISA using Rat anti-mouse IgE and biotin Rat anti-mouse IgE (Becton Dickinson Biosciences, Franklin Lakes, NJ) and performed according to manufacturer's protocol. Papain specific IgE was quantified as previously described [29]. Briefly, 96-well microtiter plates were coated overnight at 4°C with 50 μg/ml papain with c0mplete mini-protease inhibitor cocktail. The plates were then blocked with 1x casein for 1 hour, and incubated with sample overnight at 4°C. The plates were then washed, and probed with 2 μg/ml biotin Rat anti-mouse IgE for 1 hour, washed and incubated with streptavidin-HRP for 30 minutes. Plates were washed again and developed with TMB substrate, treated with 1N HCl, and read spectrophotometrically at an absorbance of 450 nm.

Statistical analysis

Results depict average±SEM. Statistical significance was determined by two-tailed unpaired T test with equal variance. Statistical significance was considered to be $P<0.05$. Results were analyzed with the use of the statistical software Prism 6 (GraphPad La Jolla, CA).

Results

NALF cytology

To evaluate the inflammatory response induced by enzymatically active papain, we analyzed the NALF cytology and compared HP and papain treated mice. NALF from papain treated mice exhibited about a 4-fold increase in lavage total cellularity (Figure 1b). Much of this increase was contributed by eosinophil influx which increased by roughly 129-fold ($p<0.001$) in papain treated mice compared to the HP treated group (Figure 1b). This demonstrates that enzymatically active papain induces a robust eosinophilic inflammatory response as seen in eosinophilic rhinosinusitis patients.

Papain promotes goblet cell hyperplasia

Goblet cell hyperplasia is a characteristic of the "weep and sweep" response during type 2 immune responses [30]. This refers to the increased mucus production and mucociliary clearance needed to clear the airway of environmental irritants and pathogens. Unsurprisingly, this IL-4/IL-13 dependent feature is also a typically exhibited in eosinophilic rhinosinusitis[3]. To analyze goblet cell populations, sinonasal histological sections from mice treated with papain and HP were stained with alcian blue (Figure 2a). Goblet cells, identified as alcian blue positive cells, were counted along the nasal septum. Indeed, we

found that papain treated mice exhibited a statistically significant 3-fold increase in septal goblet cells ($p<0.01$) (Figure 2b). This result indicates that papain treatment induces goblet cell hyperplasia in the sinonasal epithelium.

IL-33 secretion is induced by papain

We hypothesized that the observed induction of type 2 inflammation was due to protease-induced damage to the sinonasal epithelium. Proteolytic damage to the sinonasal epithelium is known to induce the release of the alarmin IL-33 [18, 31, 32]. IL-33 potently activates a variety of cell types involved in initiating and propagating type 2 responses such as type 2 innate lymphoid cells (ILC2s), mast cells, basophils, and Th2 cells [33]. Thus, we analyzed IL-33 concentrations in NALF 2 hours following HP or papain treatment. Papain treated mice exhibited a significant increase in IL-33 in NALF compared to HP treated mice indicating that intranasal instillation of papain promotes dysregulation of IL-33 release ($p<0.0001$) (Figure 3).

Flow cytometric immunophenotyping

To more comprehensively characterize the cellular infiltrate induced by papain exposure, we next analyzed sinonasal tissue by flow cytometry. Using the papain model, papain exposure increased infiltration of eosinophils, T cells, basophils, ILC2s, and mast cells in sinonasal tissue (Figure 4–5). This demonstrates activation of type 2 innate immune effectors such as basophils, ILC2s, and mast cells in conjunction with adaptive mechanisms which are T cell and B cell dependent. This combination of innate and adaptive immune effectors is representative of the inflammatory infiltrate seen in eosinophilic rhinosinusitis [3].

Papain stimulates the production of type 2 cytokines

The type 2 cytokines IL-4, IL-5, and IL-13 orchestrate type 2 immune responses by promoting IgE class switching, stimulating eosinophil differentiation from myeloid progenitors in bone marrow, and inducing mucus production, respectively [34]. We therefore sought to analyze the levels of these cytokines from sinonasal tissue homogenates of mice treated with HP and papain. Papain treated mice demonstrated a significant elevation in IL-4 ($p<0.05$), IL-5 ($p<0.01$), and IL-13 ($p<0.01$) compared to HP treated mice (Figure 6). These datasuggest that papain induces type 2 inflammatory responses via canonical IL-4, IL-5, and IL-13 dependent pathways.

IL-13 producing cells

To determine the sources of type 2 cytokines in response to papain challenge, we next analyzed IL-13 producing cell populations by intracellular staining and flow cytometry. We found a significant increase in IL-13 competent ILC2s, T cells, eosinophils, and basophils in papain treated mice as compared to HP treatment (Figure 7). These results indicate that papain stimulates activation and recruitment of innate and adaptive immune cells that are capable of producing IL-13 and maintaining a local type 2 cytokine milieu.

Nasopharyngeal associated lymphoid tissue re-stimulation

In secondary lymphoid tissues, the initiation and maintenance of adaptive immune responses requires a type 2 cytokine milieu in order to generate antigen specific T cells and IgE [35]. To determine if this phenomenon occurred in response to papain treatment, we isolated NALT, which is the draining lymphoid tissue of the sinonasal mucosa, and re-stimulated *in vitro* with inactivated papain. NALT from papain treated mice demonstrated significantly elevated production of IL-4 and IL-5 (Figure 8). However, we found a non significant increase in IL-13, which is consistent with its role as a mucosal tissue-associated cytokine [36]. This indicates the presence of papain-specific Th2 cells in the NALT of papain treated mice.

IgE production

The typical type 2 immune response is characterized by class switching of B cells to produce antigen specific IgE. IgE binds its high affinity receptor FcεRI on mast cells and basophils to promote their release of inflammatory mediators and proteases in response to antigen. Total IgE and papain specific IgE levels were quantified in serum. Indeed, we found that both total and papain specific IgE were significantly elevated in papain treated mice (Figure 9).

Discussion

Current medical and surgical interventions may fail to control ECRS disease progression and patients' quality of life. Advances in therapeutics for ECRS have been hindered by the lack of reliable experimental animal models. Effective animal models would allow for the dissection of molecular mechanisms involved in the disease pathogenesis and facilitate the identification of potential therapeutic targets. Though animal models of ECRS exist, they fail to recapitulate the complex interplay between the innate and adaptive immune mechanisms which drive the pathophysiology associated with ECRS and eosinophilic disease [3, 5, 37].

This study establishes a protease inducible murine model of eosinophilic rhinosinusitis which will facilitate further study into the underlying pathophysiology of ECRS and provide a platform for the testing of novel therapeutics. We demonstrate that intranasal instillation of papain induces the release of the epithelial derived alarmin IL-33, which is associated with epithelial injury. We show that repeated treatment with papain induces type 2 inflammatory responses characterized by ILC2 recruitment, goblet cell hyperplasia, eosinophilic infiltration, local and central type 2 cytokine production, and IgE production. These hallmarks of type 2 inflammation closely resemble the pathology seen in the sinonasal tissue of ECRS patients.

This protease inducible model offers multiple advantages in comparison to existing animal models of ECRS. A significant advantage of this model is the physiologically relevant route of sensitization via the airway epithelium. Current models such as ovalbumin, SEB and aspergillus sensitize via the intraperitoneal route [4, 27, 38]. Sensitization in this manner can bypass many of the innate pathways such as epithelial injury and innate cell activation which characterize ECRS pathology [3].

Existing models that utilize common environmental allergens, have the disadvantage of activating allergen-specific immune signaling pathways such as antifungal systems [11]. Papain, however, is not associated with any fungal molecular patterns such as β-glucans, and therefore bypasses these mechanisms. This is significant because the β-glucan-induced dectin signaling mechanisms have not, to date, been implicated in ECRS pathophysiology. Thus, allergen-induced models may not effectively capture the innate immune activation that occurs in ECRS.

Several non-murine models of ECRS have been previously reported as well. These models are typically conducted in sheep or rabbits which have sinonasal anatomy that is more similar to humans that of rodents. Rodents lack human-like paranasal sinuses, and therefore, do not necessarily develop rhinosinusitis. The advantage to a murine model, however, is the powerful genetic manipulations which are available for use in mice which facilitate future mechanistic studies into ECRS pathophysiology.

Significantly, we demonstrate that our papain-inducible model generates substantial ILC2 recruitment to the sinonasal mucosa. Recent studies have demonstrated that ILC2s are markedly elevated in sinonasal tissue in ECRS [39, 40]. To our knowledge, no existing models of ECRS have described local ILC2 recruitment. The major advantage of this model, therefore, is that it generates a Th2 phenotype comparable to those of existing models while accurately recapitulating the innate immune characteristics of ECRS. Thus, this model provides a unique experimental system in which innate immune mechanisms may be further dissected and targeted for potential therapeutics. Another advantage to the use of papain is its immunogenicity. Ovalbumin, which is used in most eosinophilic rhinosinusitis models, is not inherently immunogenic. As a result, extended challenge with ovalbumin may lead to immunological tolerance and induction of regulatory T cells [41]. In contrast, papain promotes the release of the innate type 2 epithelial cytokine, IL-33. This causes the release of so called “danger-signals” which promote inflammatory responses. As a result, this papain induced model could be extended indefinitely in order to analyze the physiologic responses which resulting from chronic type 2 inflammation in the sinonasal mucosa.

This model, however, is not without its limitations. A common characteristic of ECRS progression is the development of polypoid lesions. In this protease-induced model, although we looked at an early time course, we did not observe any polypoid lesions as have been described in the SEB model [6]. In order to better evaluate polyp progression and pathophysiology, the SEB model may be a better experimental system. Additionally, papain has limited relevance to ECRS in humans. Many common human allergens, however, demonstrate intrinsic protease activity which is essential to their immunogenicity [31, 32]. Therefore, this model provides a valuable, physiologically relevant experimental system to study eosinophilic rhinosinusitis pathophysiology. This will permit a useful model system to identify potential therapeutic targets and test.

Conclusion

This protease inducible murine model of type 2 sinonasal inflammation provides an excellent experimental platform to dissect molecular mechanisms involved in ECRS

pathophysiology and to investigate novel molecular targets for potential anti-inflammatory therapies for ECRS. This study also establishes an effective flow cytometric gating scheme to analyze type 2 inflammatory processes of the sinonasal mucosa. Therefore, this study, although observational in nature, lays the groundwork for future mechanistic studies of ECRS and eosinophilic diseases of the upper respiratory tract.

Acknowledgments

Funding sources: NIH ES020859 (to M.R.)

NIH AI072502 (A.P.L.)

References

1. Fokkens WJ, et al. EPOS 2012: European position paper on rhinosinusitis and nasal polyps 2012. A summary for otorhinolaryngologists. Rhinology. 2012; 50(1):1–12. [PubMed: 22469599]
2. London NR Jr, Tharakan A, Ramanathan M Jr. The Role of Innate Immunity and Aeroallergens in Chronic Rhinosinusitis. Adv Otorhinolaryngol. 2016; 79:69–77. [PubMed: 27466848]
3. Schleimer RP. Immunopathogenesis of Chronic Rhinosinusitis and Nasal Polyposis. Annu Rev Pathol. 2017; 12:331–357. [PubMed: 27959637]
4. Mendiola M, et al. Characterization of a novel high-dose ovalbumin-induced murine model of allergic sinonasal inflammation. Int Forum Allergy Rhinol. 2016; 6(9):964–72. [PubMed: 27060366]
5. Debeuf N, et al. Mouse Models of Asthma. Curr Protoc Mouse Biol. 2016; 6(2):169–84. [PubMed: 27248433]
6. Kim DW, et al. Staphylococcus aureus enterotoxin B contributes to induction of nasal polypoid lesions in an allergic rhinosinusitis murine model. Am J Rhinol Allergy. 2011; 25(6):e255–61. [PubMed: 22185735]
7. Hong SL, et al. Interleukin-17A-induced inflammation does not influence the development of nasal polyps in murine model. Int Forum Allergy Rhinol. 2015; 5(5):363–70. [PubMed: 25754984]
8. Kouzaki H, et al. Endogenous Protease Inhibitors in Airway Epithelial Cells Contribute to Eosinophilic Chronic Rhinosinusitis. Am J Respir Crit Care Med. 2017; 195(6):737–747. [PubMed: 27779422]
9. Steelant B, et al. Impaired barrier function in patients with house dust mite-induced allergic rhinitis is accompanied by decreased occludin and zonula occludens-1 expression. J Allergy Clin Immunol. 2016; 137(4):1043–1053 e5. [PubMed: 26846377]
10. Yu S, et al. Derp1-modified dendritic cells attenuate allergic inflammation by regulating the development of T helper type1(Th1)/Th2 cells and regulatory T cells in a murine model of allergic rhinitis. Mol Immunol. 2017; 90:172–181. [PubMed: 28802126]
11. Ito T, et al. Dectin-1 Plays an Important Role in House Dust Mite-Induced Allergic Airway Inflammation through the Activation of CD11b+ Dendritic Cells. J Immunol. 2017; 198(1):61–70. [PubMed: 27852745]
12. Cohen NR, et al. Innate recognition of cell wall beta-glucans drives invariant natural killer T cell responses against fungi. Cell Host Microbe. 2011; 10(5):437–50. [PubMed: 22100160]
13. Khalmuratova R, et al. Induction of nasal polyps using house dust mite and Staphylococcal enterotoxin B in C57BL/6 mice. Allergol Immunopathol (Madr). 2016; 44(1):66–75. [PubMed: 26242569]
14. de Migliavacca RO, et al. An experimental model of chronic rhinosinusitis in rabbits without bacterial inoculation. Acta Cir Bras. 2014; 29(5):313–9. [PubMed: 24863319]
15. Liang KL, et al. Developing a rabbit model of rhinogenic chronic rhinosinusitis. Laryngoscope. 2008; 118(6):1076–81. [PubMed: 18388772]

16. Thomas DC, Wormald PJ. Standardization of diagnostic criteria for eosinophilic chronic rhinosinusitis in the Oestrus ovis infected sheep model. Am J Rhinol. 2007; 21(5):551–5. [PubMed: 17999788]
17. Zhang F, et al. A novel model of invasive fungal rhinosinusitis in rats. Am J Rhinol Allergy. 2013; 27(5):361–6. [PubMed: 23816783]
18. Paris G, et al. Damage-associated molecular patterns stimulate interleukin-33 expression in nasal polyp epithelial cells. Int Forum Allergy Rhinol. 2014; 4(1):15–21. [PubMed: 24574111]
19. Tharakan A, et al. Reversal of cigarette smoke extract-induced sinonasal epithelial cell barrier dysfunction through Nrf2 Activation. Int Forum Allergy Rhinol. 2016; 6(11):1145–1150. [PubMed: 27580429]
20. London NR Jr, et al. Air pollutant-mediated disruption of sinonasal epithelial cell barrier function is reversed by activation of the Nrf2 pathway. J Allergy Clin Immunol. 2016; 138(6):1736–1738 e4. [PubMed: 27576127]
21. London NR Jr, et al. Nuclear erythroid 2-related factor 2 activation inhibits house dust mite-induced sinonasal epithelial cell barrier dysfunction. Int Forum Allergy Rhinol. 2017; 7(5):536–541. [PubMed: 28151586]
22. Wise SK, et al. Interleukin-4 and interleukin-13 compromise the sinonasal epithelial barrier and perturb intercellular junction protein expression. Int Forum Allergy Rhinol. 2014; 4(5):361–70. [PubMed: 24510479]
23. Wawrzyniak P, et al. Regulation of bronchial epithelial barrier integrity by type 2 cytokines and histone deacetylases in asthmatic patients. J Allergy Clin Immunol. 2017; 139(1):93–103. [PubMed: 27312821]
24. Florsheim E, et al. Integrated innate mechanisms involved in airway allergic inflammation to the serine protease subtilisin. J Immunol. 2015; 194(10):4621–30. [PubMed: 25876764]
25. Takeda T, et al. Platelets constitutively express IL-33 protein and modulate eosinophilic airway inflammation. J Allergy Clin Immunol. 2016; 138(5):1395–1403 e6. [PubMed: 27056266]
26. Morita H, et al. An Interleukin-33-Mast Cell-Interleukin-2 Axis Suppresses Papain-Induced Allergic Inflammation by Promoting Regulatory T Cell Numbers. Immunity. 2015; 43(1):175–86. [PubMed: 26200013]
27. Cho SH, et al. Spontaneous eosinophilic nasal inflammation in a genetically-mutant mouse: comparative study with an allergic inflammation model. PLoS One. 2012; 7(4):e35114. [PubMed: 22509389]
28. Heritage PL, et al. Comparison of murine nasal-associated lymphoid tissue and Peyer's patches. Am J Respir Crit Care Med. 1997; 156(4 Pt 1):1256–62. [PubMed: 9351630]
29. Sokol CL, et al. A mechanism for the initiation of allergen-induced T helper type 2 responses. Nat Immunol. 2008; 9(3):310–8. [PubMed: 18300366]
30. Madden KB, et al. Role of STAT6 and mast cells in IL-4-and IL-13-induced alterations in murine intestinal epithelial cell function. Journal of Immunology. 2002; 169(8):4417–4422.
31. Kale SL, et al. Cockroach protease allergen induces allergic airway inflammation via epithelial cell activation. Sci Rep. 2017; 7:42341. [PubMed: 28198394]
32. Snelgrove RJ, et al. Alternaria-derived serine protease activity drives IL-33-mediated asthma exacerbations. J Allergy Clin Immunol. 2014; 134(3):583–592 e6. [PubMed: 24636086]
33. Lloyd CM. IL-33 family members and asthma - bridging innate and adaptive immune responses. Curr Opin Immunol. 2010; 22(6):800–6. [PubMed: 21071194]
34. Gour N, Wills-Karp M. IL-4 and IL-13 signaling in allergic airway disease. Cytokine. 2015; 75(1): 68–78. [PubMed: 26070934]
35. Kim HY, DeKruyff RH, Umetsu DT. The many paths to asthma: phenotype shaped by innate and adaptive immunity. Nat Immunol. 2010; 11(7):577–84. [PubMed: 20562844]
36. Van Dyken SJ, et al. A tissue checkpoint regulates type 2 immunity. Nat Immunol. 2016; 17(12): 1381–1387. [PubMed: 27749840]
37. Lane AP. The role of innate immunity in the pathogenesis of chronic rhinosinusitis. Curr Allergy Asthma Rep. 2009; 9(3):205–12. [PubMed: 19348720]

38. Khalid AN, et al. Physiologic alterations in the murine model after nasal fungal antigenic exposure. Otolaryngol Head Neck Surg. 2008; 139(5):695–701. [PubMed: 18984266]

39. Mjosberg JM, et al. Human IL-25- and IL-33-responsive type 2 innate lymphoid cells are defined by expression of CRTH2 and CD161. Nat Immunol. 2011; 12(11):1055–62. [PubMed: 21909091]

40. Hulse KE. Immune Mechanisms of Chronic Rhinosinusitis. Curr Allergy Asthma Rep. 2016; 16(1):1. [PubMed: 26677109]

41. Yiamouyiannis CA, et al. Shifts in lung lymphocyte profiles correlate with the sequential development of acute allergic and chronic tolerant stages in a murine asthma model. Am J Pathol. 1999; 154(6):1911–21. [PubMed: 10362818]

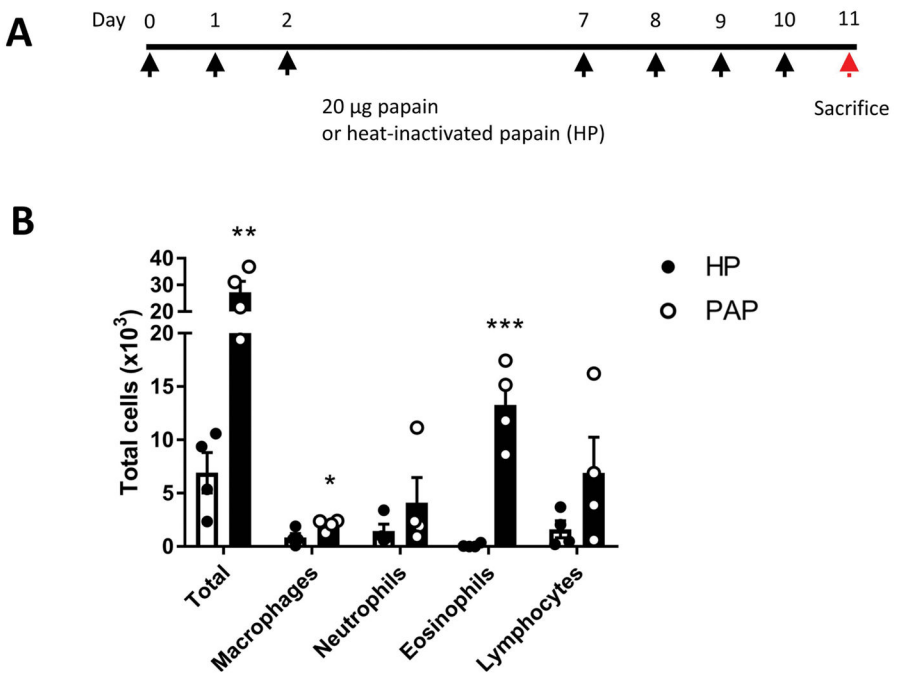

Figure 1.

Cysteine protease papain induces eosinophilic inflammation in sinonasal mucosa. (A) Schematic diagram of papain treatment course. (B) Inflammatory cell counts in NALF. Total cells were counted manually using a hemocytometer. Differential cells counts were performed on cytospin slides stained with Diff-Quick staining kit. Data is presented as mean ±SEM. **p<0.01, ***p<0.001

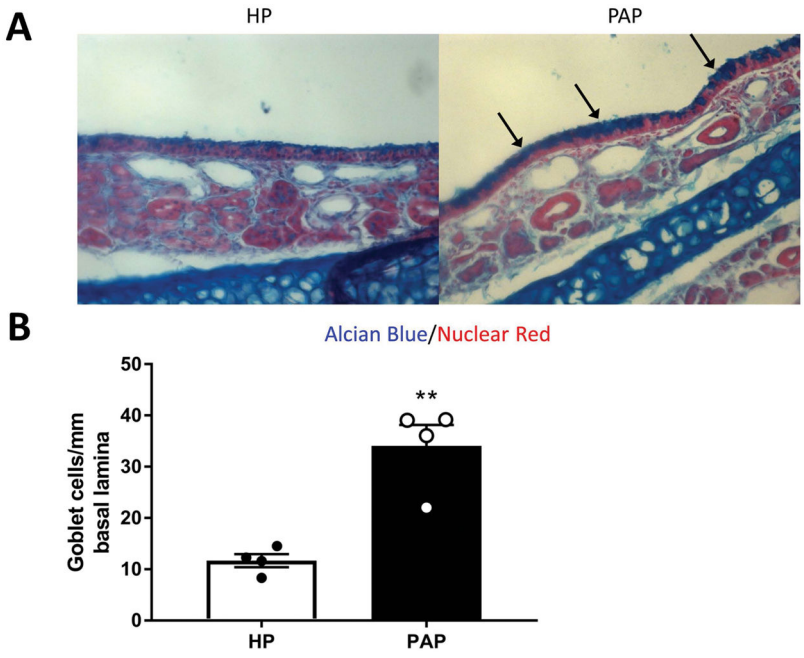

Figure 2.

Goblet cell hyperplasia following repeated papain exposure. (A) Representative photomicrograph of alcian blue stained histological sections from HP treated (left) or papain treated (right) mice. (B) Goblet cells were counted along the nasal septum and normalized per mm of basal lamina. Data is presented as mean±SEM. **p<0.01.

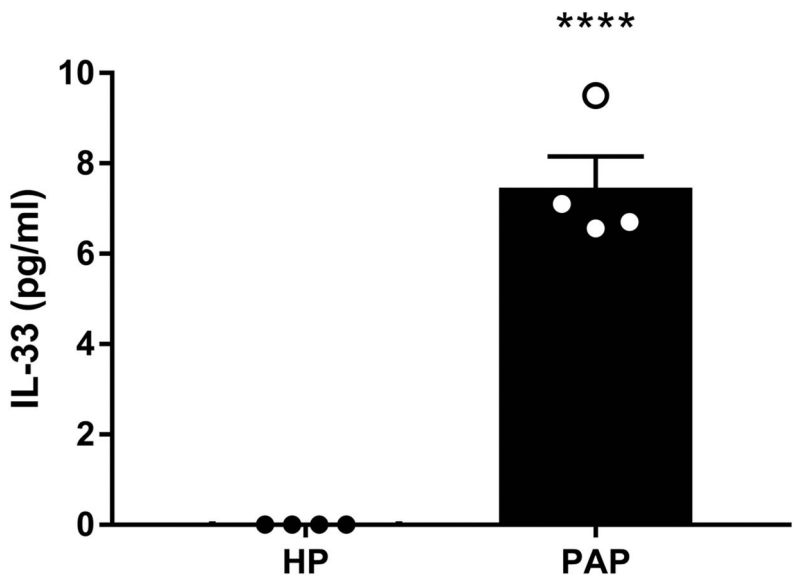

Figure 3.

Papain causes IL-33 release from sinonasal epithelial cells. IL-33 levels were quantified from NALF two hours following HP or papain treatment. Data is presented as mean±SEM. ****p<0.0001

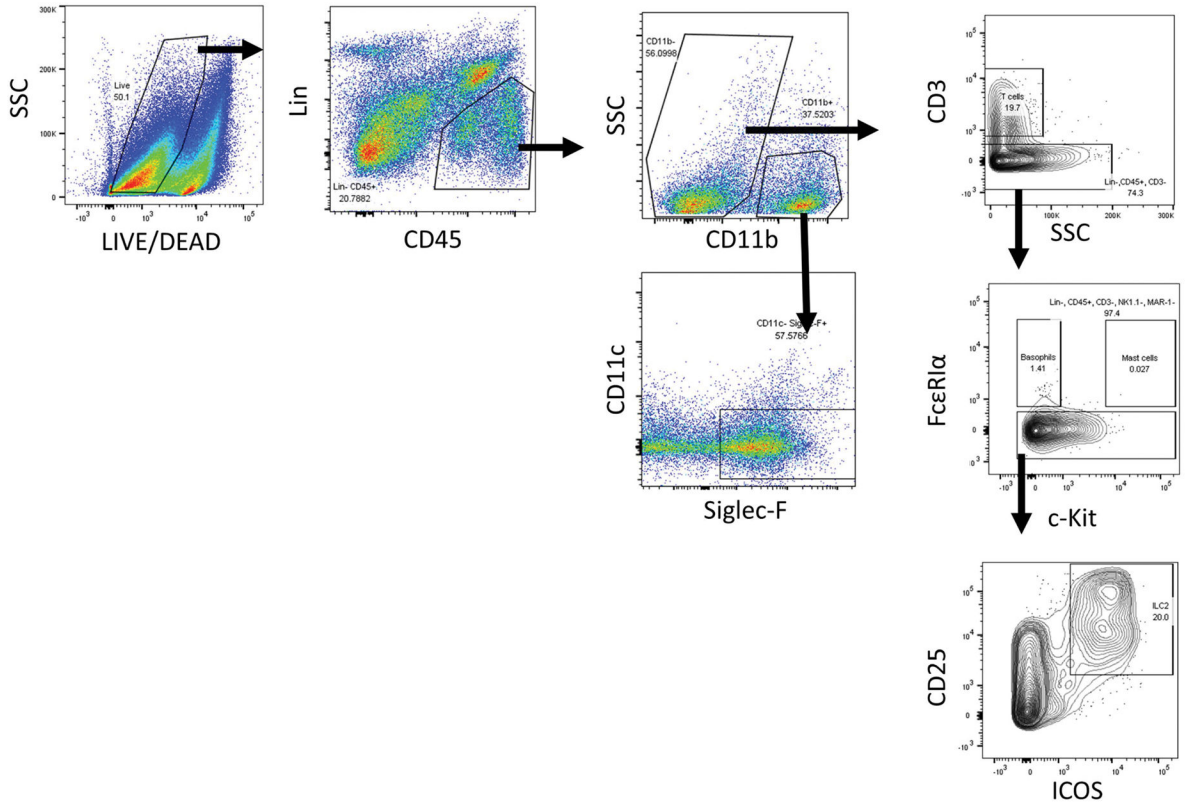

Figure 4.

Flow cytometric gating scheme for identification of immune cell influx in sinonasal tissue. Eosinophils (Lin$^-$, CD45$^+$, CD11b$^+$, CD11c$^-$, and Siglec-F$^+$) T cells (Lin$^-$, CD45$^+$, CD11b$^-$, CD3$^+$), basophils (Lin$^-$, CD45$^+$, CD3$^-$, FcεRIα$^+$, c-Kit$^-$), mast cells (Lin$^-$, CD45$^+$, CD3$^-$, FcεRIα$^+$, c-Kit$^+$), and ILC2s (Lin$^-$, CD45$^+$, CD3$^-$, CD11b$^-$, FcεRIα$^-$, c-Kit$^-$, CD25$^+$, ICOS$^+$) were identified as shown. Identification of other cell types such as neutrophils (Lin$^-$, CD45$^+$, CD11b$^+$, Gr-1$^+$), macrophages (CD45$^+$, CD11c$^+$, F4/80$^+$), B cells (CD45$^+$, B220$^+$), NK cells (Lin$^-$, CD45$^+$, NK1.1$^+$), monocyte derived dendritic cells (Lin$^-$, CD45$^+$, CD11b$^+$, CD11c$^+$, MHCII$^+$) and NKT cells (Lin$^-$, CD45$^+$, NK1.1$^+$, CD3$^+$) were identified by a different gating scheme not shown.

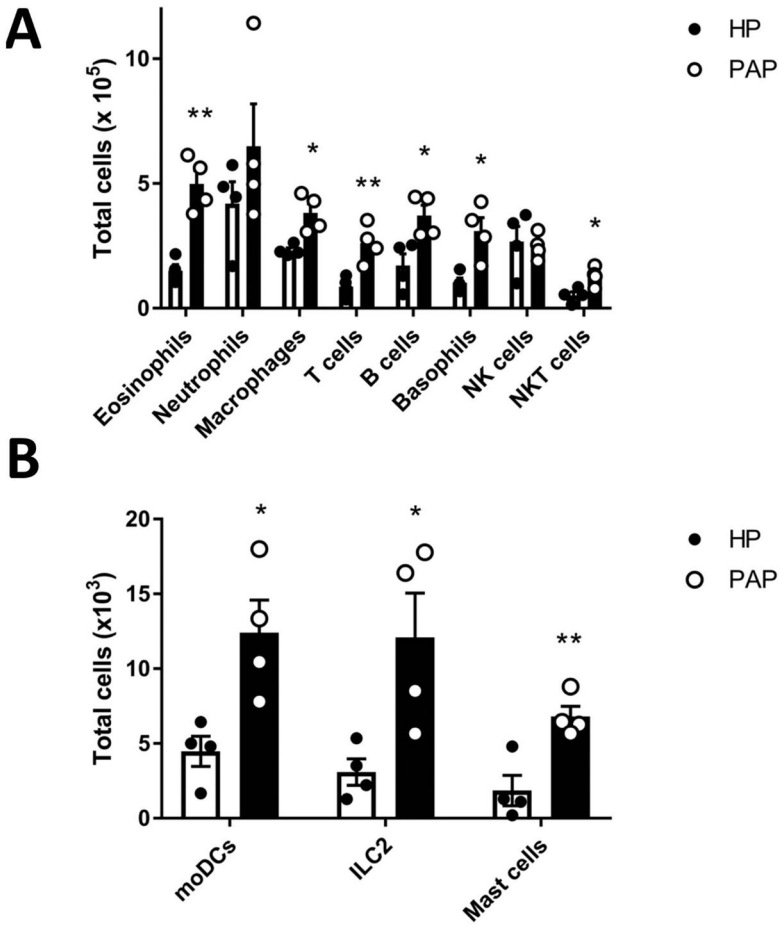

Figure 5.

Flow cytometric immunophenotyping of sinonasal tissue. (A) Total numbers of eosinophils, neutrophils, interstitial macrophages, T cells, B cells, basophils, NK cells, and NKT cells in sinonasal tissue isolated from HP and papain treated mice. (B) Total numbers of monocyte derived DCs, ILC2s, and mast cells in sinonasal tissue isolated from HP and papain treated mice. Data represented mean±SEM. *p<0.05, **p<0.01.

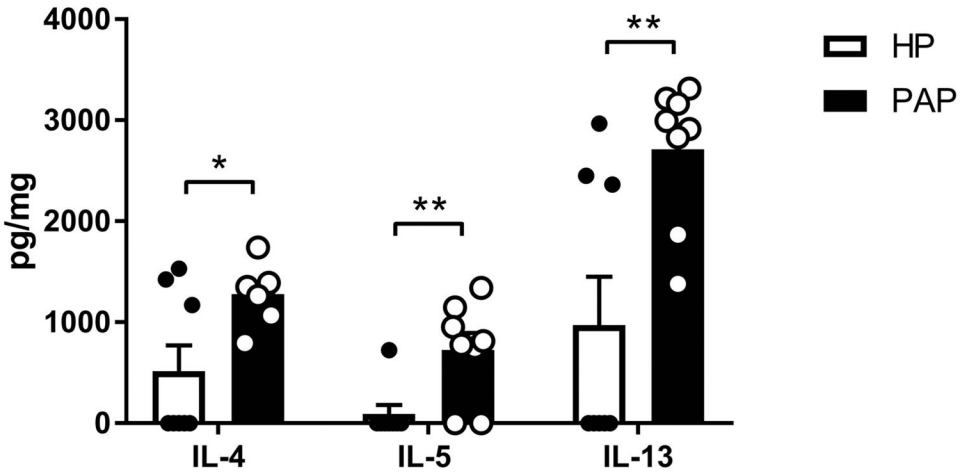

Figure 6.

Local type 2 cytokine production is induced by papain exposure. Concentrations of IL-4, IL-5, and IL-13 in sinonasal tissue homogenates. Data represented mean±SEM. *p<0.05, **p<0.01

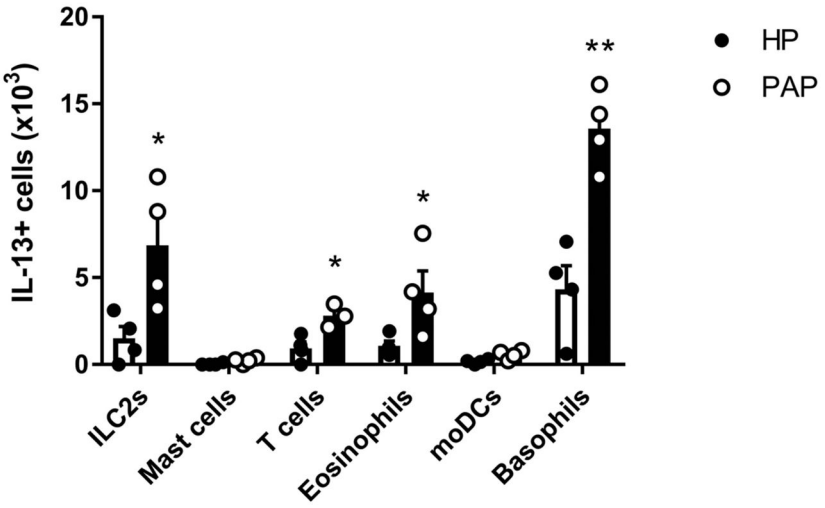

Figure 7.

Papain induces expansion and recruitment of IL-13 producing cell populations. IL-13 producing cell were analyzed by flow cytometry. Data represented mean±SEM. *p<0.05, **p<0.01

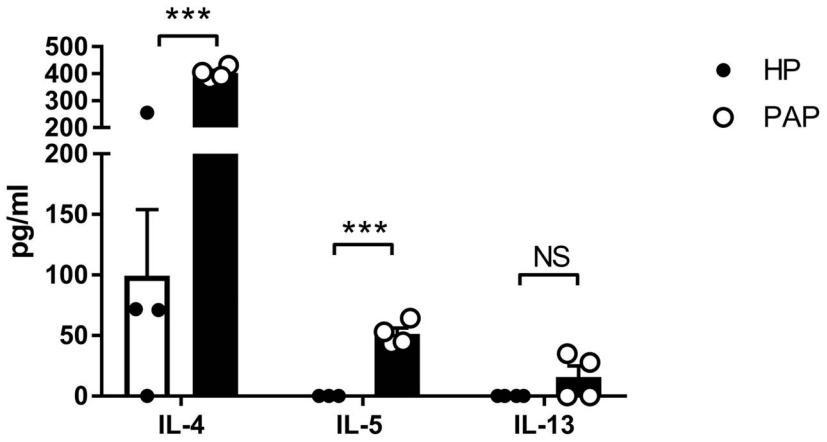

Figure 8.

Repeated papain challenges promote central Th2 polarization. Cells isolated from NALT from HP and papain treated mice were re-stimulated with inactivated papain for 3 days and cytokine secretion was analyzed. Data represented mean±SEM. ***p<0.001.

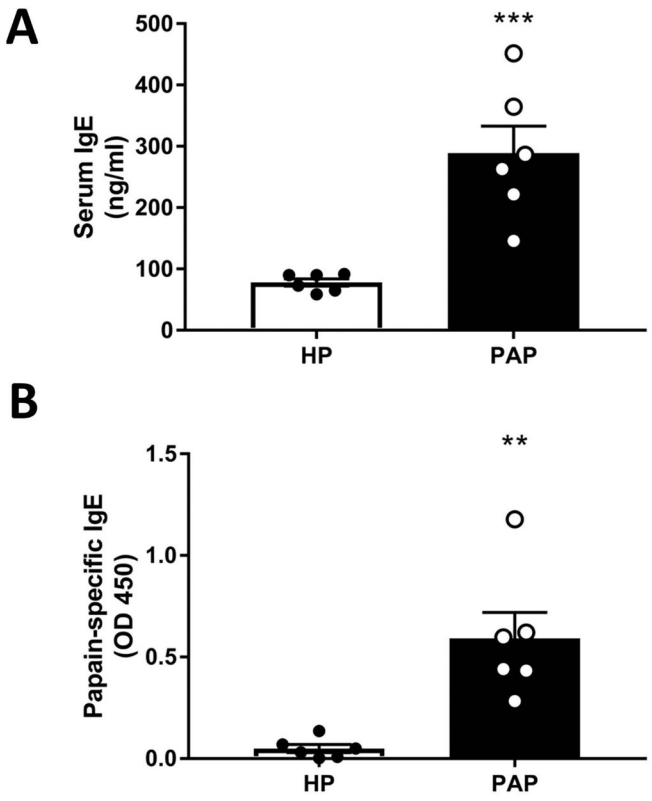

Figure 9.

B cells secreted IgE in response to papain treatment. IgE levels were quantified from serum of HP and papain treated mice. Data represented mean±SEM. **p<0.01, ***p<0.001.